

Dear Reviewer #1:

Thank you for your comments and suggestions. Those comments are all valuable and very helpful for revising and improving our paper, as well as the important guiding significance to our researchers. We have studied comments carefully and have made correction which we hope meet with approval. Now I response the comments with a point by point. Full details of the files are listed. We sincerely hope that you find our response and modifications satisfactory and that the manuscript is now acceptable for publication.

Responds to the reviewer's comments:

Comment 1: Grammar errors should be noted (e.g. in abstract Lines 10-11: the nonlinear amplitude-frequency characteristics of the test system IS analyzed...). Please check.

Response 1:

We agree with the comment and thanks for pointing out our grammar errors. In addition to fixing the errors in comment 1, we have also checked the rest of the text. The contents of the modification are as follows:

- (1) Lines 10-11: the nonlinear amplitude-frequency characteristics of the test system **are** analyzed theoretically based on the nonlinear vibration theory.
- (2) Lines 49,52,205,285: Revise “effect” to “**effects**”.
- (3) Lines 60-61: In the biaxial fatigue test, the additional **masses decouple** the biaxial load by seesaw, and the additional **masses are** called virtual **masses**, as shown in Fig. 1 (b). In this installation condition, the inertia force generated by the virtual **masses** only acts in the direction of an individual blade mode.
- (4) Lines 2,30,62-67,72,74,78,128,137-138,184,207-208: Revise “mass” to “**masses**”.
- (5) Lines 265: Given the roughly similar amplitudes, lower resonance **frequency results** in reduced inertial loads on the blade.

Comment 2: In Lines 43-46, authors state: “Therefore, IWES conducted further research, designed a device to convert virtual masses from translation to rotation.....” Where is the corresponding reference of this research? Please check it.

Response 2:

Thank you for pointing this out, we actually put the reference in the next sentence. However, to ensure the rigor of the article, we have adopted your suggestion to add the corresponding reference of research of IWES. The modification content is as follows:

Lines 43-46: “Therefore, IWES conducted further research, designed a device to convert virtual masses from translation to rotation, and applied it to the biaxial fatigue test which has a frequency ratio of 1:1 (Melcher et al., 2020)”

Corresponding reference:

[12] Melcher, D., Petersen, E., and Neßlinger, S.: *Off-axis loading in rotor blade fatigue tests with elliptical biaxial resonant excitation*, *J. Phys. Conf. Ser.*, 1618(5): 052010, <https://doi.org/10.1088/1742-6596/1618/5/052010>, 2020.

Comment 3: In Lines 46-47, authors state: “the inertia force generated by rotating virtual masses is different from that generated by translational virtual masses.” Please explicitly illustrate the difference between these two setups and explain its effects on inertia force. What is the motivation of studying nonlinear vibration characteristics of wind turbine blades based on Virtual mass match.

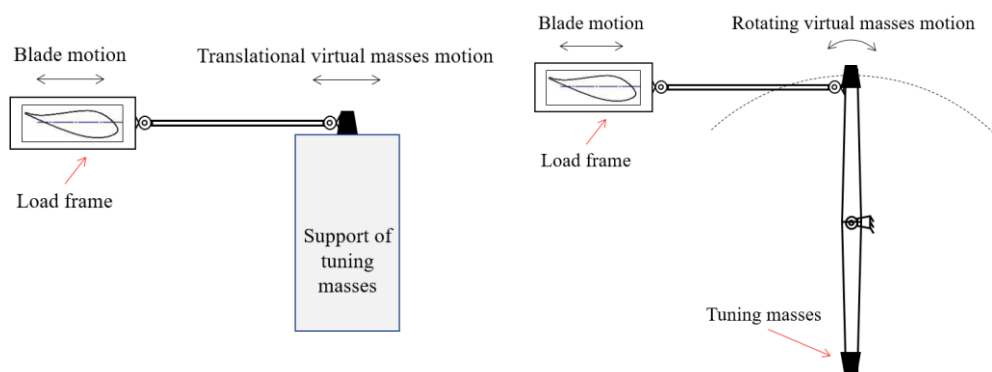
Response 3:

Thank you very much for your suggestions. We will add the explanation of text and theoretical analysis to the article. The modification content is as follows:

(1) The difference between these two setups

Add content to the original lines 46-47: “In fact, in the view of the motion characteristics, the inertia force generated by rotating virtual masses is different from that generated by translational virtual masses. The translational virtual masses move synchronously with the blade, which behave like a mass acting in just one direction from a numerical standpoint. The translational virtual masses have the same motion characteristics as the additional tuning masses. Therefore, although the virtual mass is not on the blade, the inertia force generated by it and the inertia force generated by the additional tuning masses are in the same direction and magnitude. The rotating virtual masses are limited by the constraints of the seesaw, and its motion path is the rotating motion around the center of the seesaw. Therefore, the direction and magnitude of the inertial force generated by the rotation of the virtual mass will change, and it is not equivalent to the translational virtual masses.”

If the text is not clear, it can be understood with the picture below.



Corresponding reference:

[10] Post, N. and Bürkner, F.: *Fatigue Test Design: Scenarios for Biaxial Fatigue Testing of a 60-Meter Wind Turbine Blade*, Tech. rep., National Renewable Energy Laboratory, Golden, CO, USA, <https://doi.org/10.2172/1271941>, 2016.

[17] Falko, B.: *Biaxial Dynamic Fatigue Tests of Wind Turbine Blades*, Ph.D. thesis, Leibniz University Hannover, Germany, <https://publica.fraunhofer.de/handle/publica/283519>, 2020.

(2) The explanation of the effects on inertia force

In fact, the above text (1) roughly explains that the inertia forces produced by the two setups are different because of the different motions of the virtual masses. In order to more clearly explain the effects on inertial forces between the two setups, we will add the relevant content in the section 2.1 as follows:

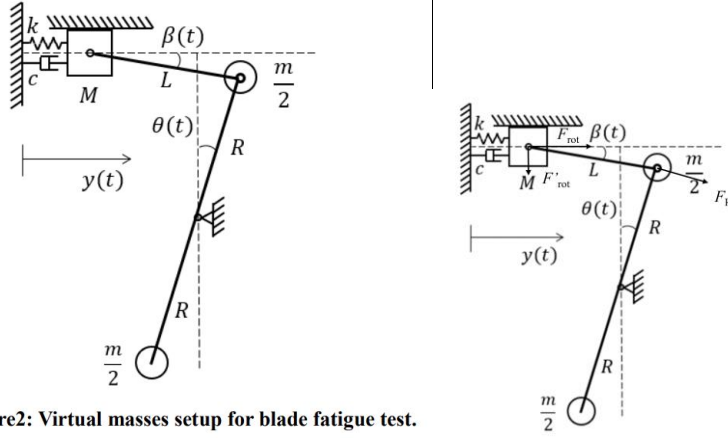


Figure2: Virtual masses setup for blade fatigue test.

According to Fig. 2, the inertial force generated by rotating virtual masses of the blade at the maximum amplitude Y can be further analyzed. The relationship of the motion between virtual mass and blade can be obtained:

$$\begin{cases} \mathbf{v}_m = \mathbf{v}_M + \mathbf{v}_{mM} \\ \mathbf{a}_m = \mathbf{a}_m^n + \mathbf{a}_m^\tau = \mathbf{a}_M + \mathbf{a}_{mM}^n + \mathbf{a}_{mM}^\tau \end{cases} \quad (n)$$

Where: \mathbf{v}_m - velocity of virtual masses; \mathbf{v}_M - velocity of blade equivalent mass; \mathbf{v}_{mM} - relative velocity; \mathbf{a}_{mM}^n - relative normal acceleration; \mathbf{a}_m - the acceleration of the virtual masses; \mathbf{a}_{mM}^τ - relative tangential acceleration; \mathbf{a}_m^n - normal acceleration; \mathbf{a}_m^τ - tangential acceleration. The blade at the maximum amplitude satisfies: $\mathbf{v}_M = 0$; $\mathbf{v}_{mM} = 0$; $\mathbf{a}_{mM}^n = 0$; $\mathbf{a}_m^n = 0$.

Depending on the direction of acceleration, Eqs. (n) can be simplified as:

$$\mathbf{a}_m^\tau = \mathbf{a}_M + \mathbf{a}_{mM}^\tau \quad (n+1)$$

The angular acceleration of the virtual mass at the maximum amplitude of the blade can be obtained:

$$|\alpha_m| = \frac{\omega^2 Y \cos(\beta_0)}{R \cos(\theta_0 - \beta_0)} \quad (n+2)$$

Where: θ - Rotation angle of the seesaw at the maximum amplitude of the blade; β_0 - Angle between the push rod and the main vibration direction at the maximum amplitude of the blade; α_m - Angular acceleration of the virtual mass at the maximum amplitude of the blade.

According to Eqs. (n+1) and Eqs. (n+2), the rotating inertia force F_R generated by the rotating virtual mass at the maximum amplitude of the blade can be obtained:

$$F_R = \frac{mR^2 \alpha_m}{R} = \frac{m\omega^2 Y \cos(\beta_0)}{\cos(\theta_0 - \beta_0)} \quad (n+3)$$

The inertia force F_{rot} transmitted to the main vibration direction of the blade through the push rod can be obtained:

$$F_{rot} = \frac{F_R \cos(\beta_0)}{\cos(\theta_0 - \beta_0)} = \frac{m\omega^2 Y \cos^2(\beta_0)}{\cos^2(\theta_0 - \beta_0)} \quad (n+4)$$

By comparison with Eqs. (8), it can be seen that the inertial force terms of two equations are same at the maximum amplitude of the blade. As mentioned above, the translational virtual masses are consistent with the motion state of the blade, so the inertial force generated by the translational virtual masses can be obtained based on Eqs. (n+3):

$$F_{tra} = m\omega^2 Y \quad (n+5)$$

According to Eqs. (n+4) and Eqs. (n+5), there are differences in the inertial forces acting on the blades by the two setups, which are mainly caused by the difference in the movement trajectory of masses.

$$\left\{ M + m \frac{\cos^2 \beta}{\cos^2(\theta - \beta)} \right\} \ddot{y} + c\dot{y} + ky + \frac{m\omega^2 \cos \beta}{\cos^4(\theta - \beta)} \left[\frac{\cos^2 \beta \sin(\theta - \beta)}{R} - \frac{\sin^2 \theta}{L} \right] = F(t) \quad (8)$$

(3) The motivation of studying nonlinear characteristics of blades based on Virtual masses match

The motivation is to adopt a reasonable control strategy for the nonlinearity brought by virtual masses to achieve the target damage in future research. In the blade-virtual masses system, the excitation equipment needs to have the function of automatic adjustment of resonance frequency to minimize the energy input, and the biaxial load (trajectory) envelope of the blade will change due to the change of resonance frequency and the influence of the virtual mass mechanism, so the blade's test specification may need to be adjusted to achieve the target damage.

We will add this motivation in the revised paper in line 47-48.

Comment 4: In Fig. 1(b), the setup of virtual masses in is different from those reported in previous works (White et al., 2004; Greaves et al., 2012; Snowberg et al., 2014; Hughes et al). It is noted that this setup introduces nonlinear terms to the test system resulting in a more complex scenario. Please explain the mechanism of the device and illustrate advantages of this device comparing with previous setups.

Response 4:

In the previous resonance biaxial test, a reasonable load distribution (in both directions) will be obtained by optimizing the position and mass of the counterweight installed on the blade. However, the tuning masses installed on the blade will affect the vibration characteristics (mode shape and frequency) in both flap-wise and edge-wise directions, which brings difficulty to the biaxial load match optimization, and there may be excessive overload in a certain area of the blade when choosing a compromise.

To simplify load match, the extra mechanism makes the tuning masses only act in one vibration direction (called virtual masses), and the biaxial load match is equivalent to the combination of the load match of two single axis test, as shown in Fig.1(b).

(1) The mechanism of the device

The mechanism for mounting the virtual mass consists of a push rod and a seesaw. The push rod, blade fixture, and seesaw are connected through a universal joint, and the seesaw can rotate around the center position. Masses are located at both ends of the seesaw to offset each other's gravity. After the exciting force is applied to the blade, the tuning masses move with the blade and rotate around the center of the seesaw to provide the inertia force for the blade.

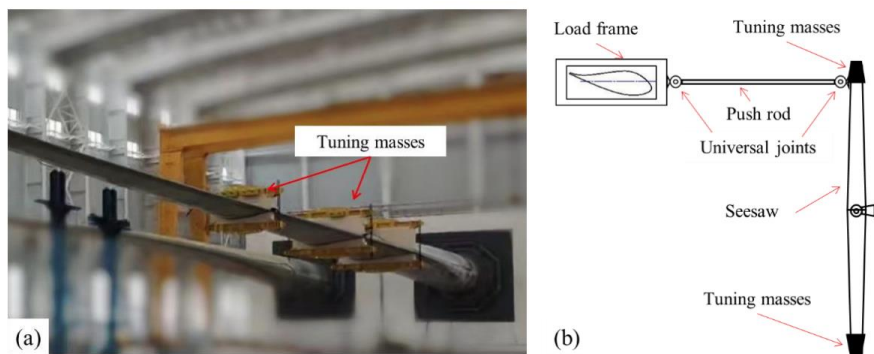


Figure 1: Masses match of blade fatigue test: (a) traditional tuning masses setup (b) virtual masses setup.

(2) Advantages of this device

- ① The virtual mass only acts in one direction, which is conducive to the decoupling of biaxial loads.
- ② This device is easier to be used in real test. In the figure of **Response 3 (1)**, it's hard to achieve translational virtual masses. Because a larger and stronger platform is needed to keep virtual mass translate, which is difficult to achieve in a limited test space. In the biaxial test, the platform may interfere with the push rod, especially when the blade has a large amplitude in the edge-wise direction.

We will emphasize mechanism of the device and advantages of this device comparing with previous setups in the revised paper.

Comment 5: In Lines 75-79, authors state: “the inertial force of the virtual masses also affects the flap-wise direction of the blade.....since the frequency of the inertial force is close to the first order modal frequency in edge-wise direction, the perturbation to the flap-wise direction is relatively small.....”. Is there any evidence (reference or theoretical analysis) supporting that the perturbation to the flap-wise direction is relatively small?

Response 5:

(1) Theoretical analysis

According to Eqs. (n+1) and Eqs. (n+2) in **Response 3** and Eqs. (8), the inertia force F'_{rot} transmitted to the secondary vibration direction of the blade through the push rod can be obtained:

$$\begin{cases} F'_{rot} = \frac{F_R \sin(\beta_0)}{\cos(\theta_0 - \beta_0)} = \frac{m\omega^2 Y \cos(\beta_0) \sin(\beta_0)}{\cos^2(\theta_0 - \beta_0)} \quad (\text{at the maximum amplitude of the blade}) \\ F'_{rot}(t) = \frac{m \cos(\beta) \sin(\beta)}{\cos^2(\theta - \beta)} \dot{y} \end{cases}$$

Taking 84m and 94m blade as an example, $R = L = 4m$, the blade amplitude in edge-wise direction is about $Y = 1m$, the selected parameters as shown in section 4.2. The proportion of perturbation in the flap-wise direction is:

$$\left(\frac{F'_{rot}}{F_{rot}} \right)_{max} = \frac{\sin(\beta_0)}{\cos(\beta_0)} = 0.032$$

Where: β_0 can be solved by Eqs. (2).

In addition, lines 76-77 state “since the frequency of the inertial force is close to the first order modal frequency in edge-wise direction”. According to the amplitude-frequency characteristic curve,

$\left(\frac{F'_{rot}}{F_{rot}} \right)_{max}$ will decrease further.

(2) Simulated analysis

Taking 84m and 94m blade as an example, $R = L = 4m$, the blade amplitude in edge-wise direction is about $Y = 1m$, the selected parameters as shown in section 4.2. From the following simulation results, the perturbation to the flap-wise direction is relatively small (0.5% of the edge-wise amplitude).

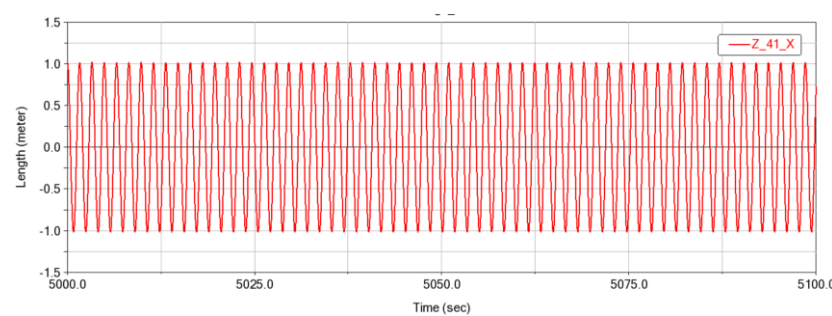


Figure: 84m blade amplitude of edge-wise direction

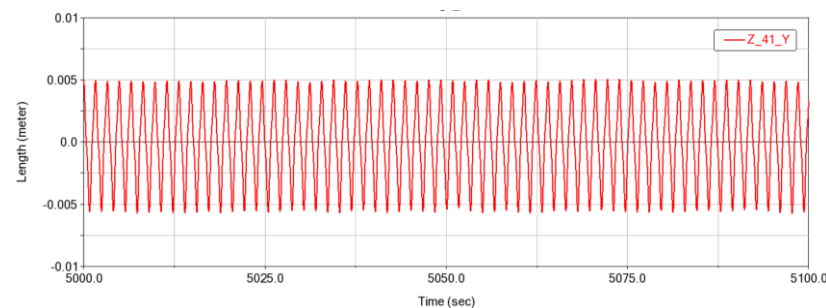


Figure: 84m blade perturbation amplitude of flap-wise direction

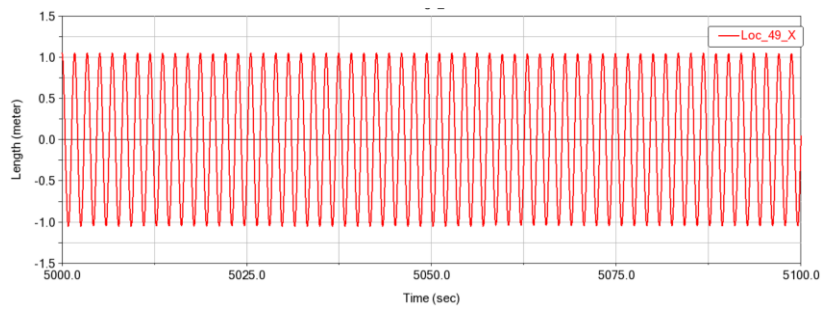


Figure: 94m blade amplitude of edge-wise direction

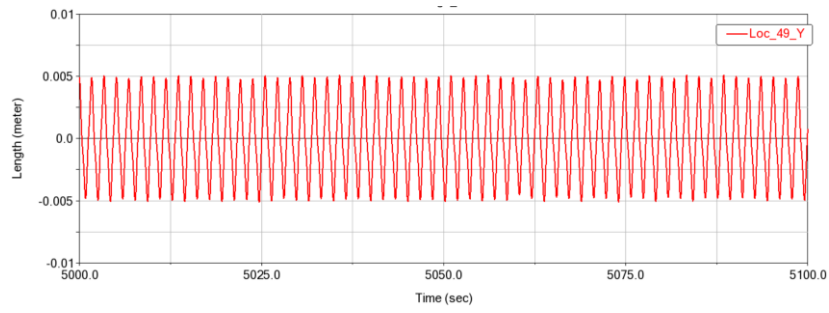


Figure: 94m blade perturbation amplitude of flap-wise direction

$$\begin{cases} T = \frac{1}{2}M(\dot{y}_f^2 + \dot{y}_e^2) + \frac{1}{2}m_f R_f^2 \dot{\theta}_f^2 + \frac{1}{2}m_e R_e^2 \dot{\theta}_e^2 \\ V = \frac{1}{2}k_f y_f^2 + \frac{1}{2}k_e y_e^2 \\ D = \frac{1}{2}c_f \dot{y}_f^2 + \frac{1}{2}c_e \dot{y}_e^2 \end{cases}$$

Some of the relevant terms in Eqs. (1) are obtained as:

$$\begin{aligned} \frac{\partial T}{\partial \dot{y}_f} &= M\dot{y}_f + \left[\frac{m_f \cos^2 \alpha_f}{\cos^2(\theta_f + \alpha_f)} + \frac{m_e \sin^2 \alpha_e}{\cos^2(\theta_e - \alpha_e)} \right] \dot{y}_f + \left[\frac{m_f \cos \alpha_f \sin \alpha_f}{\cos^2(\theta_f + \alpha_f)} - \frac{m_e \cos \alpha_e \sin \alpha_e}{\cos^2(\theta_e - \alpha_e)} \right] \dot{y}_e \\ \frac{d}{dt} \left(\frac{\partial T}{\partial \dot{y}_f} \right) &= \left[M + \frac{m_f \cos^2 \alpha_f}{\cos^2(\theta_f + \alpha_f)} + \frac{m_e \sin^2 \alpha_e}{\cos^2(\theta_e - \alpha_e)} \right] \ddot{y}_f + \left[\frac{m_f \cos \alpha_f \sin \alpha_f}{\cos^2(\theta_f + \alpha_f)} - \frac{m_e \cos \alpha_e \sin \alpha_e}{\cos^2(\theta_e - \alpha_e)} \right] \ddot{y}_e \\ &\quad + \dot{y}_f \frac{d}{dt} \left[\frac{m_f \cos^2 \alpha_f}{\cos^2(\theta_f + \alpha_f)} + \frac{m_e \sin^2 \alpha_e}{\cos^2(\theta_e - \alpha_e)} \right] \\ &\quad + \dot{y}_e \frac{d}{dt} \left[\frac{m_f \cos \alpha_f \sin \alpha_f}{\cos^2(\theta_f + \alpha_f)} - \frac{m_e \cos \alpha_e \sin \alpha_e}{\cos^2(\theta_e - \alpha_e)} \right] \end{aligned}$$

Comment 7: The amplitude-frequency curves are incomplete with their peak points missing. From this figure, it can be observed that saddle node bifurcation occurs. Does the existence of saddle node bifurcation have effects on the results of biaxial fatigue test when the dynamic characteristics of such a system differ from those of the linear system?

Response 7:

Thank you very much for pointing out these problems, our response is as follows:

(1) The amplitude-frequency curves are incomplete with their peak points missing

The peak point is missing because the amplitude of the blade is different under different damping ratios. When the damping ratio is very small, the blade amplitude is very large, so the peak point is not displayed in the existing coordinate axis range. We will modify this issue in the revised paper and choose the damping ratio appropriately to ensure a complete curve.

(2) Effects of saddle node bifurcation on the results of biaxial fatigue test

Figure 5 shows the influence of different small parameters on the amplitude-frequency characteristics of the system. In fact, specific small parameter values mean specific working conditions, that is, when the virtual mass related parameters (such as L 、 R 、 m) are determined, the amplitude-frequency characteristics of the system will also be determined. Therefore, as long as the setups are determined, the dynamic characteristics of the test system will be determined, whether it is a single axis test or a biaxial test.

In addition, the amplitude hopping phenomenon, also known as dynamic bifurcation, also appears in Figure 5. In the simulation example, we can see that the resonance frequency changes in a relatively small range (The maximum variation of resonance frequency is about 2%), and the target amplitude of the tuning mass position in the fatigue test will not be large, so there will be no obvious dynamic bifurcation in fatigue test.

Comment 8: In Lines 200-202, authors state: “modal analysis is carried out and compared with the transfer-matrix method (TMM) and test data.....” But there is no description about transfer-matrix method or the test. Please check.

Response 8:

Thank you very much for pointing out these problems, we will add the following to the revised paper in section 3.2.

Add content to the original lines 200-201: “To ensure the applicability of the model, modal analysis is carried out and compared with the transfer-matrix method (TMM) and the test data, taking the calculation of the flap-wise direction as an example, as shown in Table 1. The transfer matrix method is an approximate theoretical method used to calculate the natural frequencies and modes of systems with chain structures. The transfer matrix method separates the structure with inertia and elasticity and obtains the relationship between the discrete elements. The natural frequencies and modes of the systems can be solved according to the boundary conditions. The transfer matrix method belongs to the physical discrete method of continuous system, which is suitable for numerical solution of blade model. The three blades in Table 1 were all subjected to actual modal tests, and the obtained frequency data are obtained from the frequency domain analysis of actual test data. The actual blade modal test was carried out by hammer method.”

We will make corresponding changes in the future revised paper and try our best to improve the manuscript. These changes will not influence the content and framework of the paper. Please do not hesitate to contact us if there are any questions. We appreciate for your hard work, and hope that the correction will meet with approval. Once again, thank you very much for your comments and suggestions.

Yours sincerely,
Jinlei Shi